Heliyon 10 (2024) e28235

Contents lists available at ScienceDirect

Heliyon

journal homepage: www.cell.com/heliyon

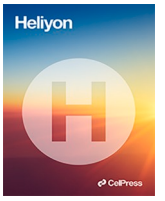

Research article

Improved empirical mode decomposition bagging RCSP combined with Fisher discriminant method for EEG feature extraction and classification

Dongyi Chen

College of Electrical Engineering and Automation Fuzhou University, NO.2, Wulong Jiangbei Avenue, Fuzhou University Town, Minhou, Fuzhou City, Fujian Province, China

A R T I C L E I N F O

Keywords:
Electro encephalon graph (EEG)
Feature extraction and classification
Improved empirical mode decomposition
Bagging RCSP
Fisher discriminant analysis

A B S T R A C T

Background: Traditional Common Spatial Pattern (CSP) algorithms for Electroencephalogram (EEG) signal classification are sensitive to noise and can produce low accuracy in small sample datasets.

New method: To solve the problem, an improved Empirical Mode Decomposition (EMD) Bagging Regularized CSP (RCSP) algorithm is proposed. It filters EEG signals through improved EMD, inhibits high-frequency noise, retains effective information in the characteristic frequency band, and uses Bagging algorithm for data reconstruction. Feature extraction is performed with regularization of spatial patterns and Fisher linear discriminant analysis for feature classification. T-test is used for classification.

Results: The improved EMD Bagging RCSP algorithm has improved accuracy and robustness compared to CSP and its derivatives. The average classification rate is increased by about 6%, demonstrating the effectiveness and correctness of the proposed algorithm.

Comparison with existing methods: The proposed algorithm outperforms CSP and its derivatives by retaining effective information and inhibiting high-frequency noise in small sample EEG datasets.

Conclusions: The proposed EMD Bagging RCSP algorithm provides a reliable and effective method for EEG signal classification and can be used in various applications, including brain-computer interfaces and clinical EEG diagnosis.

1. Introduction

Brain-Computer Interface (BCI) is a method that records brain activity through electroencephalogram (EEG) signals and decodes and analyzes them to generate commands for controlling external devices [1]. Research on motor imagery EEG signals is a major focus of BCI [2]. Motor imagery signals are EEG signals associated with specific brain activities related to a particular event, typically generated through mental imagery [3]. Studies on motor imagery have shown that during unilateral physical movement or mental imagery processes, there is a phenomenon of power spectral density attenuation or enhancement in specific frequency bands, such as α waves (8–13 Hz) and β waves (14–30 Hz), known as event-related desynchronization (ERD) and event-related synchronization (ERS) [4,5]. Based on this phenomenon, various algorithms have been designed to extract feature information from different types of motor

E-mail address: 2023fzucdy@sina.com.

https://doi.org/10.1016/j.heliyon.2024.e28235
Received 4 November 2023; Received in revised form 12 March 2024; Accepted 14 March 2024
Available online 20 March 2024

imagery signals [6]. Among them, Common Spatial Pattern (CSP) is a spatial filter suitable for binary classification, which constructs optimal spatial filters to maximize the variance differences of multichannel gait signal matrices and obtain distinct feature vectors [7–9].

The shortcomings of the CSP method lie in its weak resistance to noise interference [10]. Suppressing noise is an important approach to improving the accuracy of CSP [11]. There are various methods available for noise suppression, such as Spatially Sparse CSP, Regularized CSP, Filter Bank CSP and so on [12]. Among them, the optimal method is Regularized CSP [12]. The main idea of this method is to leverage the theory of transfer learning to organically integrate the electroencephalogram (EEG) signals of the subject with those of other subjects [13]. By incorporating the EEG signals of other subjects into the CSP learning process of the subject, the estimation bias of the subject's EEG signal covariance is guaranteed, particularly in EEG data collection experiments with small sample sizes [14]. Compared to traditional CSP, this algorithm performs better. However, the stability of this algorithm is not high, as the classification accuracy of Regularized CSP decreases and the time consumption increases when the training samples increase [15].

Fisher linear discriminant analysis is a projection method that projects points from a high-dimensional space to a low-dimensional space, which is easy to distinguish between different types of phenomena [16]. Fisher linear discriminant analysis can be used to remove the redundant features of the action to be discriminated, and it is an effective method to highlight the distinction between actions [17].

To compensate for the shortcomings of Regularized CSP, this study proposes a Bagging Regularized CSP algorithm that combines improved Empirical Mode Decomposition (EMD). This algorithm filters the multi-channel EEG signals using improved EMD signal filtering to effectively suppress high-frequency noise and ensure the preservation of relevant information within the EEG signals in the target frequency band (low-frequency band). Additionally, this algorithm constructs EEG data packets by repeatedly selecting samples and extracts RCSP features from each new data packet separately. To validate the effectiveness of this algorithm, it is compared and analyzed against RCSP and its derivative algorithms. The experimental results demonstrate that the Bagging Regularized CSP algorithm, combined with improved EMD, consistently achieves higher recognition rates and stability under low time consumption experimental conditions, outperforming RCSP and its derivative algorithms. Finally, the classified EEG signals after feature extraction are subjected to Fisher Linear Discriminant Analysis (FLDA), and the results show that this algorithm can accurately classify two types of motor imagery EEG signals.

2. Methods

2.1. Improved EMD of EEG signals

The EEG signal is a nonlinear and non-stationary signal, and the frequency of the EEG signal is mainly concentrated in the low frequency part. The application of EMD method can effectively decompose and reduce the noise of the signal, so as to obtain accurate EEG signal.

EMD is a new method proposed by Huang et al., which is suitable for processing nonlinear and non-stationary signals [18]. In essence, the signal is stabilized. The complex signal is decomposed into a finite number of Intrinsic Mode functions (IMF). The EMD method has adaptive signal decomposition and noise reduction capabilities without any prior knowledge.

When nonlinear and nonstationary EEG signals are subjected to traditional EMD, the resulting Intrinsic Mode Functions (IMFs) contain spurious low-frequency components and limited-order IMFs. To obtain EEG signals that retain the characteristic information while being free from high-frequency interference noise, an improved EMD algorithm is proposed in this article. This algorithm overcomes the limitations of traditional EMD decomposition in analyzing low-frequency EEG signals and thus achieves accurate EEG signal extraction.

2.1.1. Energy moment ratio

The energy ratio of each IMF component at different levels to the total energy of the EEG signal is calculated. By comparing the ratios, IMF components with higher ratios are selected, while spurious components are filtered out.

In Equation (1), E_i represents the energy of each IMF component, and in Equation (2), T represents the ratio of the energy E_i of each IMF component to the total energy of the EEG signal:

$$E_i = \sum_{k=1}^{n} c_i^2(k)\ i = 1, 2, \cdots, m \tag{1}$$

$$T = [E_1\ E_2\ E_3 \ldots E_m] \Big/ \sum_i E_i * 100\% \tag{2}$$

In the equation: k represents the total number of sampling points; m represents the number of IMF component; the energy moment of each order IMF component is represented as E_i; n represents the length of the time series; and the IMF component is expressed as $c_i(k)$.

2.1.2. Variance contribution rate

The variance contribution rate is introduced to highlight the relative importance of each order of Intrinsic Mode Function (IMF) component. Equation (3) reveals that the larger the value of M_i, the more significant the corresponding order of IMF component is in

the original signal.

$$M_i = D_i \Big/ \sum_{i=1}^{m} D_i \tag{3}$$

and $D_i = \frac{1}{n}\sum_{k=1}^{n} c_i^2(k) - \left[\frac{1}{n}\sum_{k=1}^{n} c_i(k)\right]^2 \; i = 1, 2, \cdots, m.$

In the equation: M_i represents the variance contribution rate of each order of IMF; $C_i(k)$ denotes the i-th IMF component; D_i represents the variance of the i-th IMF component; n represents the length of the time series; m represents the number of IMF component.

2.1.3. Decomposition and reconstruction of brain electric signals

The nonlinear and non-stationary brain electric signal x(k) is decomposed into a series of Intrinsic Mode Functions (IMFs) $c_i(k)$ and a residual component $r_n(k)$, which have finite orders and contain temporal scale information. This decomposition is represented by Equation (4).

$$x(k) = \sum_{k=1}^{n} c_i(k) + r_n(k) \; i = 1, 2, \cdots, m \tag{4}$$

The selected useful IMF components are then reconstructed into the reconstructed signal of the brain electric signal using Newton interpolation method.

2.2. Bagging RCSP algorithm

The Bagging RCSP algorithm inherits the algorithmic concept of transfer learning from RCSP-A, which involves incorporating electroencephalographic (EEG) data from other subjects into the covariance matrix of a specific subject's EEG signal. The algorithm excels in effectively preserving individual differences and capturing common features in EEG signals. Traditional RCSP lacks stability under small sample experimental conditions, as the increase in the number of training samples leads to a decrease in classification accuracy and an increase in computational time complexity. This paper proposes the use of the Bagging approach, which involves repeatedly selecting training data samples to form data bags. By incorporating partial EEG data from other subjects into the RCSP algorithm to calculate the covariance matrix of the subject's signal, new feature components are derived using RCSP based on this covariance matrix [18].

2.2.1. The covariance matrix of the participants' electroencephalogram (EEG) signals

The covariance matrix of the participants' electroencephalogram (EEG) signals is established based on the EEG signals of the participants. Assuming matrix $D_{N\times T}$ represents the EEG signals, with N channels and T samples per channel. The normalized covariance matrix and the average of the covariance matrix are represented by Equations (5) and (6) respectively:

$$C = \frac{DD^T}{tr\left(DD^T\right)} \tag{5}$$

$$\overline{C_i} = \frac{1}{M}\sum_{m=1}^{M} C_{\{\mathrm{i,m}\}} \tag{6}$$

Here, i represents the classification of motor imagery, which includes left-hand and right-hand motor imagery. M represents the number of training samples.

2.2.2. Covariance matrix estimation based on Bagging-RCSP

D_{left} and D_{right} represent the $N \times T$-dimensional EEG signal matrices (with subscripts left and right representing left-hand and right-hand motor imagery respectively) after improved Empirical Mode Decomposition (EMD). N represents the number of channels, and T represents the number of samples per channel. According to Equation (5), the spatial covariance after standardization of D_{left} and D_{right} is C_{left} and C_{right} respectively.

$$C_{left} = \frac{D_{leftr}D_{left}^T}{tr\left(D_{left}D_{left}^T\right)} \tag{7}$$

$$C_{right} = \frac{D_{right}D_{right}^T}{tr\left(D_{right}D_{right}^T\right)} \tag{8}$$

The various types of regularized average spatial covariance matrices are calculated using RCSP as follows:

$$S_i(\beta,\gamma) = (1-\gamma)X_i(\beta) + \frac{\gamma}{\beta} tr(X_i(\beta)) \times I \tag{9}$$

where β and γ are two regularization parameters ($0 \le \beta, \gamma \le 1$) and β, representing the weight values of the training sample covariance matrix to reduce the estimation bias of the covariance matrix. γ represents the weight for multiple identity matrices, and I represents the $N \times N$ identity matrix. The subscript i takes the values 1 and 2, representing the two classes of matrices corresponding to left and right-hand motor imagery, respectively. $X_i(\beta)$ represents the covariance matrix of specific subjects and the covariance matrix of the EEG data of other subjects, as expressed by the following equation:

$$X_i(\beta) = \frac{(1-\beta) \times C_i + \beta \times C_i^{'}}{(1-\beta) \times M + \beta \times M^{'}} \tag{10}$$

where C_i represents the covariance matrix composed of M training data of class for a subject, and $C_i^{'}$ represents the covariance matrix composed of $M^{'}$ training data of class for other subjects. The introduction of this term aims to obtain more reliable classification results by reducing the variance of the covariance matrix estimation.

The diagonalization decomposition of the covariance matrix in Equations (7)–(10) yields Equation (11) as below:

$$S = \overline{S_{left}} + \overline{S_{right}} = U_0 \sum U_0^T \tag{11}$$

$\overline{S_{left}}$ and $\overline{S_{right}}$ represent the composite average of the covariance matrix, $\sum$ represents the eigenvalue matrix, and U_0 represents the eigenvector matrix related to $\sum$.

Since the composite covariance matrix S is a positive definite matrix, it can be decomposed using the singular value decomposition theorem. After arranging the eigenvalues in descending order, the whitening matrix can be obtained: $P = \sum^{-1/2} U_0^T$.

The average of the covariance matrix can be transformed as follows:

$$Q_{left} = P\overline{S_{left}}P^T \tag{12}$$

$$Q_{right} = P\overline{S_{right}}P^T \tag{13}$$

Q_{left} and Q_{right} have common eigenvectors. There exist two diagonal matrices $\sum_{left}$ and $\sum_{right}$, as well as the same eigenvector matrix B. After performing principal component decomposition on Equations (12) and (13), we obtain Equations (14)–(16):

$$Q_{left} = B\sum\nolimits_{left} B^T \tag{14}$$

$$Q_{right} = B\sum\nolimits_{right} B^T \tag{15}$$

$$\sum\nolimits_{left} + \sum\nolimits_{right} = I \tag{16}$$

Analysis reveals that when Q_{left} has the maximum eigenvalue, Q_{right} corresponds to the minimum eigenvalue. Hence, matrix B can be used for classifying binary problems. The projection matrix W is represented as $W = {U_0}^T P$. W serves as a spatial filter, where the original electroencephalogram (EEG) signal $D(t)$ is projected onto a new dataset Z_0 after applying the spatial filter W, as shown in Equation (17):

$$Z_0 = D(t) \cdot W \tag{17}$$

Matrix $Z = [z_1, z_2, \cdots, z_{2m}] \in R^{N \times 2m}$ is constructed by combining the first m ($m < \frac{T}{2}$) rows and the last m rows of Z_0. Therefore, the eigenvector $f = [f_1, f_2, \cdots, f_{2m}]^T \in R^{2m \times 1}$ is defined, where f_i is specified as follows:

$$f_i = \log\left(\frac{\mathrm{var}(z_i)}{\sum_{j=1}^{2m} \mathrm{var}(z_j)}\right), i = 1, 2, \cdots, 2m$$

Finally, FLDA is utilized to map the eigenvectors to a lower-dimensional space for the classification of left and right-hand motor imagery.

2.3. Fisher discriminant analysis (FLDA) for EEG signal classification

The main idea of FLDA is to obtain the optimal projection axis using dimensionality reduction techniques, maximizing the between-class distance and minimizing the within-class distance. This allows for significant differentiation between two classes of signals. In this paper, it is proposed to apply FLDA for linear discriminant classification of feature vectors after obtaining the optimal spatial filter W through Common Spatial Patterns (CSP). The reconstructed EEG signals are then filtered using the spatial filter. The filtered matrix is denoted as Z, as shown in Equation (18):

$$Z_{N\times T} = w_{N\times N} \cdot E_{N\times T} \tag{18}$$

In the equation, E represents the reconstructed EEG signal data, where N is the number of channels and T is the number of sampling points for each channel. w denotes the optimal feature spatial filter.

From the filtered matrix $Z_{N\times T}$, feature space matrix f_p is extracted and defined as:

$$f_p = \log\left(\mathrm{var}(Z_p) \Big/ \sum_{i=1}^{2m} \mathrm{var}(Z_i)\right)$$

where Z_p is composed of k rows selected from the matrix Z before and after filtering. The aforementioned feature space matrix is then used in the Fisher algorithm.

First, the mean vector $m_j(j = 1, 2)$ representing the feature vectors of the two classes of data is calculated using Equation (19), where subscript 1 represents left-hand motor imagery and subscript 2 represents right-hand motor imagery. The within-class distance S_w is the sum of variances of the two datasets and is represented by Equation (20).

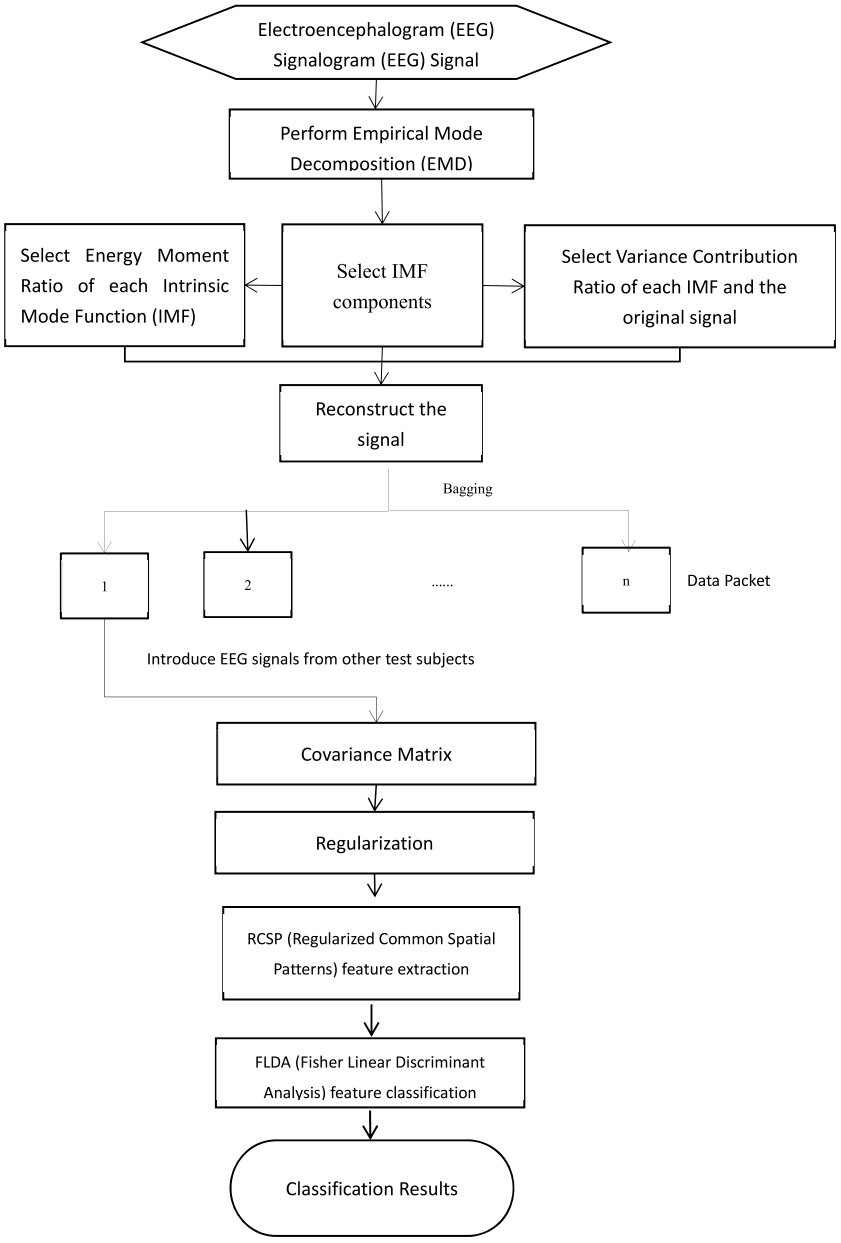

Fig. 1. The process of classifying brain electrical signals.

$$m_j = \frac{1}{N_j}\sum_{X \in f_{pj}} X \tag{19}$$

$$S_w = \sum_{j=1}^{2}\sum\nolimits_{X \in f_{pj}} (X - m_i)(X - m_i)^T \tag{20}$$

In the equation, N_j represents the number of data points of different class feature vectors, and f_{pj}, and $X \in f_{pj}$.

Additionally, the inter-class distance S_b is calculated using Equation (21):

$$S_b = (m_1 - m_2)(m_1 - m_2)^T \tag{21}$$

Furthermore, the projection matrix A^* is obtained using Equation (22):

$$A^* = S_w^{-1}(m_1 - m_2) \tag{22}$$

Finally, the EEG data is projected onto the normal vector A^* to obtain $y = (A^*)^T X$.

In order to further verify the effectiveness of FLDA dimensionality reduction method and reflect its significant dimensionality reduction effect, this method was compared with the Principal Component Analysis (PCA) dimensionality reduction method.

PCA reduces the dimensionality of feature space through linear combination of features, and the dimensionality is linearly independent. PCA first removes dimensional features with small variance by calculating variance, because the size of variance between feature dimensions is positively proportional to the amount of information it represents. The greater the variance, the greater the importance rate of the information represented. In order to reduce dimension, the feature dimension with small variance should be removed from high dimension to low dimension.

2.4. The process of classifying brain electrical signals

The process of classifying brain electrical signals is illustrated in Fig. 1. Firstly, the brain electrical data is subjected to improved Empirical Mode Decomposition (EMD) filtering. The resulting meaningful Intrinsic Mode Function (IMF) components are reconstructed to obtain the denoised brain electrical signals. Feature extraction is performed on the denoised signals using Bagging-RCSP. Finally, the brain electrical data is classified based on the extracted features using Fisher Linear Discriminant Analysis (FLDA). The specific classification process is depicted in Fig. 1.

2.5. Introduction to EEG data sets

2.5.1. Dataset1

Dataset1 originates from the BCI Competition IV dataset IIa. This dataset primarily comprises EEG signals recorded from nine subjects (A01, A02, …, A09) participating in four different motor imagery tasks: left hand, right hand, feet, and tongue, prompted by cues on a computer screen. Each subject underwent recording over two days, with each day consisting of two sessions and each session composed of six runs. The dataset1 is bifurcated into two principal components: training and testing, each encompassing 288 trials. Every category of motor imagery data incorporates 72 trials, with 22 EEG signal sampling channels and a device sampling rate set at 250 Hz. This research focused on the EEG data for two distinct motor imagery tasks, the left and right hand, downsampled to 100 Hz for algorithm verification. A total of 144 trials of left- and right-hand motor imagery data were extracted from the dataset1, with 42 trials from each category designated for training data and the remainder utilized for testing.

2.5.2. Dataset2

Dataset2 is derived from the BCI Competition III (2005) dataset IVa, which primarily includes the motor imagery EEG data of five healthy subjects (aa, al, av, aw, ay). These EEG data comprise channel data from 118 leads, with a signal acquisition frequency of 100 Hz and a total of 280 samples per subject. Each subject executed three types of motor imagery tasks (left hand, right hand, and right foot) based on visual cues. However, the competition only provided an equal quantity of right hand and right foot motor imagery data for each subject. The dataset is partitioned into training and testing categories, with five subsets of sample data (comprising 168, 224, 84, 56, and 28 samples, respectively) from the five subjects chosen for training and the remaining sample data designated for testing.

2.5.3. Dataset3

Dataset3 was obtained from the EEG data acquisition device (NeuroScan SynAmp2 8050) in the laboratory through the experiment of designing motor imagination action classification task. The dataset3 recorded 5 subjects (NORMAL06, NORMAL07, NORMAL08, NORMAL09, NORMAL10) performing left - and right-handed motor imagination tasks when prompted by left - and right-handed arrows. The task period of each experiment was 26 s, which was divided into three stages: the first stage was to rest for 1s, the second stage was to perform movement imagination for 10s, and the third stage was to rest for 15s. In each round of the experiment, the subjects were required to perform 10 consecutive experimental tasks. The paper select randomly 5 times of experimental data as training data, and the remaining 5 times of data as test data.

The three data sets are divided into training set and test set. The data in the training set is applied 10-fold cross validation, that is, the training data set is divided into ten parts, and 9 of them are trained and 1 of them is verified in turn. The average of the results of the

10 times is used as the estimation of the algorithm accuracy. After 10 times of 10-fold cross-validation, the recognition accuracy rate obtained from the test set data is expressed as the final accuracy rate.

The hardware configurations for the three data sets are shown in Table 1.

2.6. Statistical method

The T-test algorithm proposed in this paper is analyzed by using the T-test method (which is paired with double-tail detection) to compare the effective differences in the average recognition rate with the CSP, RCSP, SSCSP, FBCSP and other algorithms. If $P < 0.001$ is found, it indicates that there is a significant difference, which shows that the algorithm proposed in this paper has a strong distinction in recognition rate.

3. Results and discussion

3.1. Results and discussion of the dataset1

The main objective of this study is to select left-hand and right-hand motor imagery datasets from a larger dataset1, consisting of a total of 144 experiments. Out of these, 42 experiments from each category are randomly chosen as training data, while the remaining samples are used as testing data. In order to improve classification accuracy and reduce classification time, the proposed algorithm in this paper divides the training dataset1 of 9 participants into smaller data packets. The algorithm then selects data packets based on their correlation with classification accuracy and applies Feature Extraction using Regularized Common Spatial Patterns (RCSP) to perform data classification using Fisher's Linear Discriminant Analysis (FLDA). Comparative experiments are conducted between CSP, RCSP, SSCSP, FBCSP, and the proposed algorithm in this paper. The results of the comparison show effective differences in recognition rate and time consumption between CSP and its derivative algorithms, and the improved EMD Bagging-RCSP proposed in this paper, as shown in Table 2. The time consumption represents the total time taken for feature extraction and classification of the testing data of the 9 participants.

Compared with the data in Table 2, which is also the FLDA dimensionality reduction method, different CSP and its derivative algorithms are compared, and it can be found that the average recognition accuracy rate of the proposed algorithm is increased by more than 5%, and the sample standard deviation of the proposed algorithm is smaller than that of other algorithms, indicating that the algorithm has better algorithm robustness than other algorithms. The T-test algorithm (which is paired with double-tail detection) proposed in this paper is analyzed and compared with other algorithms. The significant differences are found at $P < 0.001$, which indicates that the algorithm proposed in this paper has strong differentiation in recognition rate. In terms of computational time, the traditional CSP algorithm has a relatively small computational load, suggesting that algorithm complexity affects the time required. However, the algorithm proposed in this study has made certain improvements in terms of computational time compared to other CSP derivative algorithms.

Considering the average recognition rate and computational time of the algorithms, it can be concluded that the algorithm proposed in this study is superior to the traditional CSP algorithm and its derivatives. The new algorithm proposed in this paper outperforms all other methods in the recognition rate of all samples.

3.2. Results and discussion of the dataset2

The main work of this study involved training on five sets of samples from the five subjects (with 168, 224, 84, 56, and 28 samples, respectively), while the remaining 840 samples were used as testing data. To improve classification accuracy and reduce classification time, the proposed algorithm in this study took advantage of the positive correlation between classification accuracy and training samples. Specifically, the large training samples were divided into smaller data packets, and then RCSP features were extracted to select data and apply FLDA for data classification. Comparative experiments revealed effective differences in recognition rates and computational time between algorithms such as CSP, RCSP, SSCSP, FBCSP and the proposed improved EMD Bagging-RCSP on this dataset, as shown in Table 3. The computational time represents the total time taken for feature extraction and classification on the remaining 840 test data from the five subjects.

Compared with the data in Table 3, which is also the FLDA dimensionality reduction method, different CSP and its derivative algorithms are compared, and it can be found that the average recognition accuracy rate of the proposed algorithm is increased by more than 5%, and the sample standard deviation of the proposed algorithm is smaller than that of other algorithms, indicating that the algorithm has better algorithm robustness than other algorithms. It is obtained by T-test algorithm that the significant differences are found at $P < 0.001$. The algorithm proposed in this paper has strong differentiation in recognition rate. It can be concluded that, based

Table 1
Hardware configurations of three data sets.

Datasets	Number of subjects	Number of channels	Sampling rate	Motor ImageryTask
Dataset1	9	22	250 Hz	Left hand、right hand
Dataset2	5	118	100 Hz	Left hand、right hand
Dataset3	5	68	1000 Hz	Left hand、right hand

Table 2
Comparison of recognition rates (%) for CSP, RCSP, SSCSP, FBCSP and the algorithm of this study on BCI Competition IV Dataset 2a.

Algorithm	1	2	3	4	5	6	7	8	9	Average ± Standard deviation	Time consumed (s)
CSP	77.6	47.9	77.4	54.7	54.6	39.4	83.3	80.8	58.0	63.7 ± 16.2	9.5
RCSP	78.8	49.3	79.7	60.1	55.1	41.2	85.7	83.1	60.8	66.0 ± 16.2	70.2
SSCSP	78.5	50.2	79.1	58.6	54.5	40.3	85.5	82.2	60.2	65.5 ± 16.2	75.8
FBCSP	76.8	45.5	76.5	61.3	56.8	42.3	83.9	81.6	60.5	65.0 ± 15.4	77.2
Algorithm of this study	80.5	57.2	82.8	71.1	60.4	50.1	87.8	85.0	65.1	71.1 ± 13.6	69.1

Table 3
Comparison of recognition rates (%) for CSP, RCSP, SSCSP, FBCSP and the algorithm of this study on BCI Competition III Dataset IVa.

Algorithm	aa	al	av	aw	ay	Average ± Standard deviation	Time consumed (s)
CSP	65.3	97.1	57.1	85.6	60.1	73.0 ± 15.6	6.5
RCSP	73.8	95.3	71.7	90.1	75.1	81.2 ± 9.6	65.3
SSCSP	72.5	96.0	68.5	88.6	74.5	80.0 ± 10.5	73.2
FBCSP	69.7	94.2	70.1	83.4	71.5	77.8 ± 9.6	80.5
Algorithm of this study	75.5	97.2	72.8	91.1	80.4	85.4 ± 9.3	61.1

on the average recognition rate and time consumption, the algorithm proposed in this paper outperforms traditional CSP and its derivative algorithms. The new algorithm proposed in this paper outperforms all other methods in the recognition rate of all samples.

3.3. Results and discussion of the dataset3

To further validate the feasibility and advantages of the proposed algorithm in this paper, a comparative experiment was conducted between the algorithm proposed in this paper and CSP, RCSP, SSCSP, FBCSP which using the left-right-hand motor imagery dataset3 collected from five participants, based on the reference data such as average recognition rate and processing time shown in Table 4.

The two types of signals corresponding to left and right-hand motor imagery are combined into one sample set. In this study, Data from 10 experiments per object were selected for feature extraction experiments. The unfiltered CSP, RCSP, SSCSP, FBCSP and improved EMD Bagging-RCSP algorithms were used for feature extraction and classification of the left and right-hand motor imagery signals, respectively. FLDA algorithm was applied to project the high-dimensional feature vector into the linear space, and then feature classification was carried out. The scatter diagram of the feature distribution of left and right hand motion imaginary EEG signals of one subject was shown in Fig. 2. There was a clear distinction between the two actions, and the same action points tended to be concentrated while the regions of different action points were scattered. The classification and recognition rates of EEG signals of 5 subjects under the last two different algorithms are shown in Table 4.

In Fig. 2, the dashed black line represents the optimal projection axis, and the solid black line represents the direction of the normal vector of the projection. From the figure, it can be observed that the EEG signals after improved EMD Bagging CSP filtering exhibit optimal projection axis on Fisher's Linear Discriminant Analysis (FLDA), enabling classification of left and right-hand motor imagery features. Further improvement in classification accuracy of different types of motor imagery can be achieved by training a large data sets of EEG signals to strengthen the feature values.

Fig. 2 represents the distribution of two classes of features after feature extraction. There is a clear discrimination between the brainwave signals associated with left and right-hand motor imagery. The improved EMD Bagging-RCSP algorithm incorporates the preprocessed brainwave signals using improved EMD filtering into the RCSP algorithm along with the brainwave data from other subjects. This reduces the bias in the estimation of the signal's covariance matrix. In the calculation process, the samples of the subjects were repeatedly selected 10 times for cross-verification, so as to extract the characteristic EEG signals of the left and right hand motor imagination with obvious differentiation and strong robustness. These features are then accurately classified using FLDA.

The average classification recognition rate for the improved EMD Bagging CSP was 86.6%. The average recognition accuracy is higher than other algorithms. By comparing the data in Table 4, which is also the FLDA dimensionality reduction method, different CSP and its derivative algorithms are compared, it can be found that the average recognition accuracy of the proposed algorithm is increased by more than 5%. The significant differences are found at $P < 0.001$ by the T-test algorithm, which indicates that the

Table 4
Classification recognition rates (%) for CSP, RCSP, SSCSP, FBCSP and the algorithm of this study.

Subjects	CSP	RCSP	SSCSP	FBCSP	Algorithm of this study
NORMAL06	77.52	80.43	79.54	80.11	87.11
NORMAL07	89.10	92.11	91.07	90.54	92.35
NORMAL08	72.48	73.14	75.05	74.25	82.51
NORMAL09	79.85	80.31	81.44	82.67	86.91
NORMAL10	77.44	78.45	79.86	79.13	84.19
Average ± Standard deviation	79.3 ± 6.1	80.9 ± 6.9	81.4 ± 5.9	81.3 ± 6.0	86.6 ± 3.7

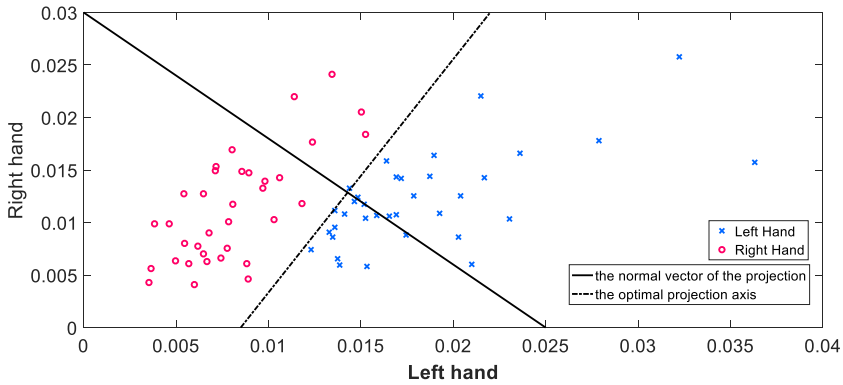

Fig. 2. Distribution map of brain electroencephalogram (EEG) signal features during left and right-hand motor imagery.

algorithm proposed in this paper has strong differentiation in recognition rate which compared with other algorithms.

In order to further verify the effectiveness of FLDA dimensionality reduction method and reflect its significant dimensionality reduction effect, this method was compared with the PCA dimensionality reduction method.

According to the data analysis in Table 5: The same bagging RCSP algorithm is applied for feature extraction, and the FLDA dimensionality reduction method is compared with PCA dimensionality reduction method. It is found that the recognition effect after FLDA dimensionality reduction is better than that after PCA dimensionality reduction, and the average recognition rate is increased by more than 6%. The T-test analysis shows that there are significant differences between the two dimensionality reduction methods. The P value was less than 0.01. The main reason is that PCA method is looking for the main axis direction that is used to effectively represent the common characteristics of the same class of samples, which has obvious advantages in representing the common characteristics of the same class of data samples. However, PCA is not suitable for distinguishing different classes of samples, and FLDA method is looking for the most effective direction for distinguishing different classes of samples. Satisfy the recognition accuracy requirement of binary classification task.

4. Conclusions

In the context of brain signal feature extraction and classification, this paper proposes a new algorithm and validates it on the BCI Competition IV dataset 2a, the BCI Competition III dataset IVa and the self-collected data set respectively. The analysis of the results shows that compared with CSP and its derivative algorithms, the algorithm proposed in this paper has a higher average recognition rate and a lower time consuming algorithm. The algorithm proposed in this paper improves the average action recognition rate by nearly 10% and saves time significantly, which proves the effectiveness and accuracy of the proposed algorithm in EEG feature extraction and classification.

The limitations of this study are as follows: 1. Compared with the existing artificial intelligence algorithms such as convolutional neural networks, the average recognition rate of EEG signals needs to be further improved, and the feature extraction and accurate classification of EEG signals under multiple classification tasks need to be further optimized. 2. The lead number of EEG acquisition channels is different. The signal coupling relationship between different channels and the method of channel dimensionality reduction are studied in this paper. It is ideal to use the fewest channels to obtain the best classification accuracy, because while ensuring the classification accuracy, the reduction of the number of channels is conducive to reducing the loss of resources, and the data processing time will also be reduced, which can speed up the actual running speed of the BCI. 3. Lack of in-depth research on the robustness of action classification accuracy on different classifiers.

Data openly available in a public repository

The dataset1 and dataset2 that support the findings of this study are openly available in http://www.bbci.de/competition.

Data availability statement

The data will be available on request to corresponding author (2023fzucdy@sina.com).

CRediT authorship contribution statement

Dongyi Chen: Writing – review & editing, Writing – original draft, Supervision, Software, Project administration, Methodology, Investigation, Formal analysis, Conceptualization.

Table 5
Classification recognition rates (%) for PCA and FLDA algorithms.

Subjects	Algorithm of this study (FLDA)	PCA
NORMAL06	87.11	80.56
NORMAL07	92.35	89.71
NORMAL08	82.51	79.25
NORMAL09	86.91	81.55
NORMAL10	84.19	73.41
Average ± Standard deviation	86.6 ± 3.7	80.9 ± 5.9

Declaration of competing interest

The author declare that he have no known competing financial interests or personal relationships that could have appeared to influence the work reported in this paper.

References

[1] J.N. Mak, J.R. Wolpaw, Clinical applications of brain-computer interfaces: current state and future prospects, IEEE Rev. Biomed. Eng. 2 (2009) 187–199.
[2] S. Kumar, A. Sharma, A new parameter tuning approach for enhanced motor imagery EEG signal classification, Med. Biol. Eng. Comput. 56 (2018) 1861–1874.
[3] G. Townsend, B. Graimann, G. Pfurtscheller, Continuous EEG classification during motor imagery-simulation of an asynchronous BCI, IEEE Trans. Neural Syst. Rehabil. Eng. 12 (2) (2004) 258–265.
[4] A. Al-Saegh, S.A. Dawwd, J.M. Abdul-Jabbar, Deep learning for motor imagery EEG-based classification: a review, Biomed. Signal Process Control 63 (2021) 102172.
[5] K. Chen, et al., NAO robot walking control system based on motor imagery, in: Journal of Physics: Conference Series, IOP Publishing, 2020.
[6] X. Zhao, et al., A multi-branch 3D convolutional neural network for EEG-based motor imagery classification, IEEE Trans. Neural Syst. Rehabil. Eng. 27 (10) (2019) 2164–2177.
[7] T. Al-Ani, D. Trad, V.S. Somerset, Signal processing and classification approaches for brain-computer interface, Intell. Biosensors 1 (2010) 25–66.
[8] G. Pfurtscheller, F.L. Da Silva, EEG-Event-Related desynchronization (ERD) and event-related synchronization, in: Electroencephalography-Basic Principles, Clinical Applications and Related Fields, Kluwer/Lippincott Williams & Wilkins, 2011, pp. 935–948.
[9] B. Graimann, B.Z. Allison, G. Pfurtscheller, Brain-computer Interfaces: Revolutionizing Human-Computer Interaction, Springer Science & Business Media, 2010.
[10] T. Liu, et al., Robust time delay estimation with unknown cyclic frequency in co-channel interference and impulsive noise, Digit. Signal Process. 117 (2021) 103166.
[11] T. Nishiura, et al., Localization of multiple sound sources based on a CSP analysis with a microphone array, Proceedings (Cat. No. 00CH37100) 2 (2000): II1053-II1056 vol.2. IEEE Int. Conf. Acoust. Speech, Signal Process. (2000), 2000. IEEE
[12] F. Lotte, C. Guan, Regularizing common spatial patterns to improve BCI designs: unified theory and new algorithms, IEEE Trans. Biomed. Eng. 58 (2) (2010) 355–362.
[13] Y.-P. Lin, T.-P. Jung, Improving EEG-based emotion classification using conditional transfer learning, Front. Hum. Neurosci. 11 (2017) 334.
[14] F. Lotte, et al., A review of classification algorithms for EEG-based brain–computer interfaces: a 10 year update, J. Neural. Eng. 15 (3) (2018) 031005.
[15] S.-H. Park, D. Lee, S.-G. Lee, Filter bank regularized common spatial pattern ensemble for small sample motor imagery classification, IEEE Trans. Neural Syst. Rehabil. Eng. 26 (2) (2017) 498–505.
[16] A. Rozza, et al., Novel Fisher discriminant classifiers, Pattern Recogn. 45 (10) (2012) 3725–3737.
[17] R. Fu, Y. Tian, T. Bao, Recognition method of single trial motor imagery electroencephalogram signal based on sparse common spatial pattern and Fisher discriminant analysis, Sheng wu yi xue gong cheng xue za zhi= J. Biomed. Eng.= Shengwu yixue gongchengxue zazhi 36 (6) (2019) 911–915.
[18] Y. Chun-Lin, C. Jun, L. Jiu-Fei, Bagging RCSP algorithm for extracting EEG feature, Acta Autom. Sin. 43 (11) (2017) 2044–2050.